LARGE SCALE NAVIER-STOKES MULTI-BODY LAUNCH VEHICLE FLOWFIELD SIMULATIONS

Johnson. C T. Wang and Stephen Taylor
Department of Computer Science, California Institute of Technology
Pasadena, CA 91125, U. S. A.

Abstract

This paper presents a large scale computational fluid dynamics (CFD) simulation of low supersonic flowfields, freestream Mach number 1.2 and the Reynolds number 2 millions per foot, over a multi-body launch vehicle system which consists of a center core and nine boosters. The full Naviers-Stokes equations, with a Baldwin-Lomax turbulent model, are solved using a finite volume numerical technique. The convective fluxes are constructed using a second order total-variation-diminishing (TVD) algorithm and the viscous fluxes, a central difference algorithm. The simulations are performed using distributed memory parallel computer systems. The essential features of the numerics and implementation are reported. for this study, 504 nodes of the Cray T3D are used. A total of 700 mega words of core memory is used. Flowfields at 5 degrees angle-of attack for rocket plumes on as well as plumes off are simulated to address the upstream effects of the rocket plumes on the flowfield and consequently, the overall aerodynamic characteristics of the entire system. The computed surface pressures agree reasonable well with the wind tunnel data. Plume-induced separations are numerically simulated; however the nature of the separation is different from those reported by previous researches. The computed center of pressure shift due to the effects of rocket plumes is also in agreement with that observed in the flight.

Introduction

Genesis The Delta II launch vehicles, made by the McDonnell Douglas, are consists of a center core and nine boosters as depicted in Figure (1). It was reported that in the first two launches, passing through transonic regime, the vehicles experienced unexpected aerodynamic characteristics which is very much different from the wind tunnel data, reference (1). A comparisons of the wind tunnel measured normal force acting on the vehicle with that of the flight is shown in Figure (2) for the case of freestream Mach number 1.2 and 5 degree angle-of-attack. The redistribution of this normal force implies that in the flight the vehicle experienced a forward (upstream) shifting of the center of pressure (cp-shift). Although there is possible that the wind tunnel data may not be accurate in the transonic regime, it is believed that the present difference between the wind tunnel data and the flight data is due to the rocket plumes in the fight, which was not simulated in the wind tunnel. It is hypothesized that this cp-shift phenomenon is caused by the plume-induced separation, as depicted in Figure (3).

Previous Works It has been recognized long time ago that the interaction of rocket or jet plumes with external flowfield over a vehicle is important to system performance, references (2) and (3). In extreme cases, plume induced separation may result in catastrophic aerodynamic instability, reference (2). In these reports, single body systems are concerned. The regions of flowfield considered are limited in the aft end of the vehicle about one core diameter upstream from the base. Reference (4) identified the important parameters in this subject. The roles played by these parameters depend on the freestream and the nozzle conditions. Therefore, it is difficulty to simulate or model using wind tunnel and analytical approach. Recently, the studies on this subject have been resorted to the solutions of the coupled Euler equations and the boundary equations or the solutions of the Navier-Stokes equations using CFD approach. The direct solution of the Navier-Stokes has become more attractive because of its uniform validity for a wide range flow speed and condition, such as complicated geometry as considered in this paper. The further attraction of the Navier-Stokes CFD method is that most of the empiricism can be avoided. Reference (5) presented an account on the recent progress of the Navier-Stokes CFD works related to this subject.

Present Studies As discussed early, previous studies on the subject of plume flowfield interaction are concentrated in the vehicle aft-end or base region. The present studies are carried out for the entire system which includes a center core and nine boosters. The so called Reynolds average Navier-Stokes equations are solved for a domain approximately 5 core diameters upstream of the vehicle tip and 20 core diameters down stream of the rocket nozzle. The simulations were carried out using a distributed memory parallel computer Cray T3D. The flow solver was massively parallelized, using domain decomposition technique, version of the ALSINS code, reference (6). The solver solves the full Navier-Stokes equations using a finite volume technique. The convective fluxes are constructed using a second order accurate total-variation-diminishing (TVD) algorithm, references (7) and (8), and the viscous fluxes, the standard central difference scheme. The development, validation, and benchmarking of the parallelized version of the code has been present in references (9) to (12). In reference (12), the flowfields over the configuration of the present study were presented for the case of zero degree angle-of-attack. The CFD simulated lamda-shock in the front of boosters and diamond-shaped flow pattern behind the overexpanded supersonic nozzles are present in comparison with the flow visualization of Van Dyke, reference (13). In the present paper, the solutions for the case of 5 degree angle-of-attack are presented. The main objective is to address the cp-shift as observed in the flight. The case of plume-off was first simulated. The CFD simulated surface pressures agree reasonably well with the available wind tunnel data. As expected, there are no flow separation in the aft-end region. The case of plume-on was then simulated. Indeed, there are flow separations, induced by the plumes, in the aft-end region. By integrating the CFD predicted surface pressure the normal force distribution and the center of pressure are obtained. By comparing the cp locations for plume-on and plume-off cases. The present study predicted a forward cp-shift in agreement with that observed in flight as reported in reference (1).

Physical Modeling

Governing Equations The flowfields simulated and presented in this paper are based on the three-dimensional Navier-Stokes equations written in conservation law form:

$$\frac{\partial U}{\partial t} + \nabla \cdot \vec{F} = 0 \tag{1}$$

where U is the vector of the conserved variables

$$U = [\rho\ \rho u\ \rho v\ \rho w\ e]^T \tag{2}$$

and F = Ee + Fe + Ge is the vector form of the fluxes of the conserved variables:

$$E = \begin{bmatrix} \rho u \\ \rho u^2 + p + \tau_{xx} \\ \rho uv + \tau_{xy} \\ \rho uw + \tau_{xz} \\ (e + p + \tau_{xx})u + \tau_{xy}v + \tau_{xz}w + q_x \end{bmatrix} \tag{3}$$

$$F = \begin{bmatrix} \rho v \\ \rho uv + \tau_{xy} \\ \rho v^2 + p + \tau_{yy} \\ \rho vw + \tau_{yz} \\ \tau_{yx}v + (e + p + \tau_{yy})v + \tau_{yz}w + q_y \end{bmatrix} \tag{4}$$

$$G = \begin{bmatrix} \rho w \\ \rho uw + \tau_{xz} \\ \rho vw + \tau_{zy} \\ \rho w^2 + p + \tau_{zz} \\ \tau_{zx}u + \tau_{zy}v + (e + p + \tau_{zz})w + q_z \end{bmatrix} \tag{5}$$

$$\begin{aligned} \tau_{xx} &= -2\mu\frac{\partial u}{\partial x} - \lambda\nabla\cdot\vec{V}, \\ \tau_{yy} &= -2\mu\frac{\partial v}{\partial y} - \lambda\nabla\cdot\vec{V}, \\ \tau_{zz} &= -2\mu\frac{\partial w}{\partial z} - \lambda\nabla\cdot\vec{V} \\ \tau_{xz} &= \tau_{zx} = -\mu\left(\frac{\partial u}{\partial z} - \frac{\partial w}{\partial x}\right), \\ \tau_{yx} &= \tau_{xy} = -\mu\left(\frac{\partial u}{\partial y} - \frac{\partial v}{\partial x}\right), \\ \tau_{yz} &= \tau_{zy} = -\mu\left(\frac{\partial v}{\partial z} - \frac{\partial w}{\partial y}\right) \\ \vec{q} &= q_x\hat{e}_x + q_y\hat{e}_y + q_z\hat{e}_z = -k\nabla T \end{aligned} \tag{6}$$

In the equations 1 to 6, ρ is the density; p is the pressure; u, v, and w are components of the velocity vector $\vec{V}$ in the x, y, and z directions, respectively, with corresponding unit vectors $\hat{e}_x$, $\hat{e}_y$, and $\hat{e}_z$. The total energy per unit volume is denoted by e; $\vec{q}$ is the heat transfer vector; T is the temperature; λ is the bulk viscosity; μ is the viscosity, and k is the thermal conductivity. The gas being assumed polytropic, the total energy is related to pressure p by the equation of state: $p = (\gamma - 1)[e - \rho(u + v + w)/2]$. The viscosity and the thermal conductivity are comprised of molecular and turbulent components as $\mu = \mu^M + \mu^T$ and $k = k^M + k^T$, respectively. Here μ^T is evaluated using a Baldwin-Lomax turbulence model, reference (14).

The equations are non-dimensionalized using the free stream pressure, density, temperature, and speed of sound.

Numerical Modeling

Numerical solutions are carried in a body confirming orthogonal curvilinear coordinate system with the transformation:

$$\xi = \xi(x, y, z); \eta = \eta(x, y, z); \zeta = \zeta(x, y, z) \qquad (7)$$

Using this set of transformation, Eqn.(1) can be written as:

$$\frac{\partial \tilde{U}}{\partial t} + \frac{\partial \tilde{E}}{\partial \xi} + \frac{\partial \tilde{F}}{\partial \eta} + \frac{\partial \tilde{G}}{\partial \zeta} = 0 \qquad (8)$$

Where

$$\tilde{U} = U/J,$$
$$\tilde{E}J = E\xi_x + F\xi_y + G\xi_z,$$
$$\tilde{F}J = E\eta_x + F\eta_y + G\eta_z,$$
$$\tilde{G}J = E\zeta_x + F\zeta_y + G\zeta_z$$

and J is the Jacobian of the transformation,

$$J = \frac{\partial(\xi, \eta, \zeta)}{\partial(x, y, z)} = \begin{vmatrix} \xi_x & \xi_y & \xi_z \\ \eta_x & \eta_y & \eta_z \\ \zeta_x & \zeta_y & \zeta_z \end{vmatrix} \qquad (9)$$

Boundary Conditions:

Far Fields: A non-reflecting boundary condition similar to that proposed by Jameson and Baker, reference (15), is applied. The equations for implementation are given in reference (6).

Solid Boundary: Non slip boundary condition for velocity is applied on the solid surface. Since the computational grids are clustered near the solid surface, the surface pressure assumes the cell center pressure of the first cell next the solid surface. Constant wall temperature, equal to the freestream temperature, is assumed.

Rocket Nozzle Exit The rocket nozzles are super sonic overexpanded.

Booster rocket exit conditions: Non-dimensionalized pressure = 0.6954; density = 0.084; and velocity = 9.725.

Core rocket exit conditions: non-dimensionalized pressure = 0.3173; density = 0.00608; and velocity = 28.2.

Numerical Results

Shown in Figure (4) is the computational grid system used in the present study. The domain of computation has been extended approximately 5 diameters upstream of the core vehicle tip and 20 core diameters downstream of the nozzle exits. There is a plane of symmetry; therefore, the simulations are carried out for half of the core and four and half of the boosters. Figures (5a) and (5b) show the pressure contours, on the pitch plane of symmetry, for the cases of plume-off and plume-on, respectively. Figures (6a)and (6b) show the comparisons of the CFD simulated surface pressure with that of the wind tunnel data for the case of plume-off. The agreements are reasonably good. The CFD did not predicted the high pressure rise. This may be caused by not having enough grid points in that region. However, this local discrepancy should not affect our main objective which is to address the cp-shift. The boosters marked by the symbol x are firing. Those without mark x are not firing. The station location, x, in relation to the vehicle configuration can be found in Figure (2). Figures (7a) and (7b) show the velocity vectors in the aft-end region, on the pitch plane of symmetry, for the cases of plume-off and plume-on, respectively. It is seen that a plume induced separation as shown in Figure (7b). It should be pointed out that the rocket as shown in figure (7b) is not firing. Therefore this is not a classical plume induced separation. Figure (8) shows the normal force distribution for the plume-on and plume-off cases. This figure qualitative similar to Figure (2). The forward cp-shift can almost be seen from this figure. Figure (9) shows the windward and leeward pressure differential. The shapes of pressure differential are similar to that of the normal force distribution. This may indicate the flow is smooth in between the boosters and the core.

Discussions

The results of a large scale computational fluid dynamics (CFD) simulation of the flowfields, for a freestream Mach number 1.2 at 5 degree angle-of attack and the Reynolds number 2 millions per foot, over a multi-body launch vehicle system which consists of a center core and nine boosters have been presented. Flowfields for rocket plumes on and plumes off are simulated to address the upstream effects of the rocket plumes on the flowfield and consequently, the overall aerodynamic characteristics of the entire system. The

computed surface pressures agree reasonable well with the wind tunnel data. Plume-induced separations are numerically simulated; however, the nature of the separation is different from that reported by previous researchers. The computed center of pressure shift due to the effects of rocket plumes is also in agreement with that observed in the flight.

References

1. Cantwell, M. N. "Delta II Transonic Aerodynamic TIM," Memo A3-L230-M-90-049, McDonnell Douglas Company, 12 March 1990.

2. Deep, R. A., Henderson, J. H., and Brazzel, C. E., "Thrust Effects on Missile Aerodynamics," U.S. Army Missile Command, RD-TR-71-9, May 1971.

3. Addy, A. L., Korst, H. H., Walker, B. J., and White, R. A., "A Study of Flow Separation in the Base Region and Its Effects During Powered Flight," AGARD-CP-124, AGARD Conference Proceedings No. 124 on Aerodynamic Drag, Specialists' Meeting, April 10-13, 1973.

4. Korst, H. H., White, R. A., Nyberg, S. E., and Agrell, J., "Simulation and Model of Jet Plumes in Wind Tunnel Facilities," AIAA j. Spacecraft, Vol. 18, No. 5, Sept.-Oct., 1981, pp427-434.

5. York, B. J., Sinha, N. and Dash, S. M. "Navier-Stokes Simulation of Plume/Vertical Launching System Interaction Flow.

6. Wang, J. C. T., and Widhopf, G. F., "An Efficient Finite Volume TVD Scheme for Steady State Solutions of the 3-D Compressible Euler/Navier-Stokes Equations". AIAA Paper 90-1523, June 1990.

7. Wang, J. C. T., and Widhopf, G. F., "A High Resolution TVD Finite Volume Scheme for Euler Equations in Conservation Form". Journal of Computational Physics, volume 84, p. 145, 1989.

8. Harten, A., "High Resolution Schemes for hyperbolic Conservation Laws". Journal of computational Physics, volume 49, p. 357, 1983.

9. Wang, J. C. T., and Taylor, S. "A Concurrent Navier-Stokes Solver for Implicit Multibody Calculations". Parallel CFD 93, Paris, France, 1993, Elsiver Press.

10. Taylor, S. Wang, J. C. T "Concurrent, Nodal Mismatched, Implicit Navier-Stokes Solver", Parallel CFD94, Kyoto Japan, 1994, Elsiver Press.

11. Taylor, S., and Wang, J. C. T. "Launch Vehicle Simulations Using a Concurrent, Implicit Navier-Stokes Solver", AIAA paper 95-0233, 33rd Aerospace Sciences Meeting, Jan., 1995. to be publish in AIAA J. Spacecraft.

12. Taylor, S., and Wang, J. C. T. "Complex Multi-Body Launch Vehicle Simulation Using A Concurrent Navier-Stokes Solver," Parallel CFD95, Pasadena USA, 1995.

13. Van Dyke, M. An Album of Fluid Motion, Parabolic Press, 1982.

14. Baldwin, B. S., and Lomax, H., "Thin Layer Approximation and Algebraic Model for Separated Flow," AIAA paper 78 - 257, 1978.

15. Jameson, A, and Baker, T. J., "Multigrid Solutions of the Eular Equations for Aircraft Configurations" AIAA paper 84-0093, Jan. 1984.

Figures

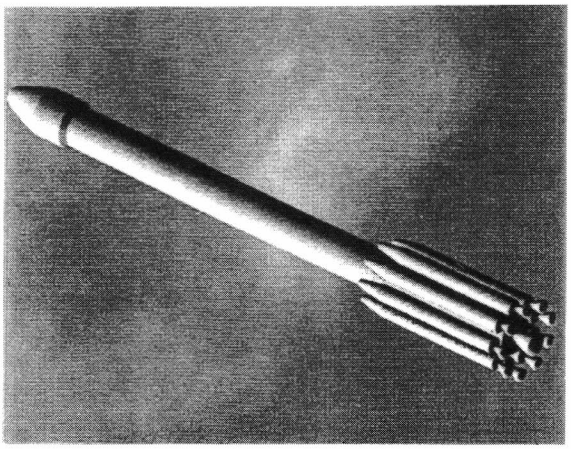

Figure (1): Multi-Body Launch Vehicle, One Center Core Plus Nine Boosters

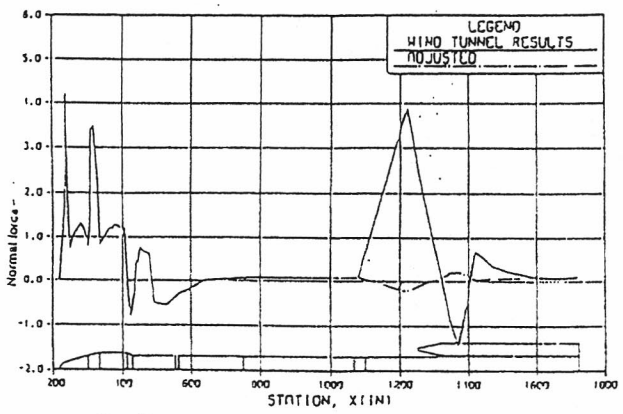

Figure (2): Normal force distribution, Mach = 1.2, alpha = 5 deg
—— wind tunnel data; —·— flight data.

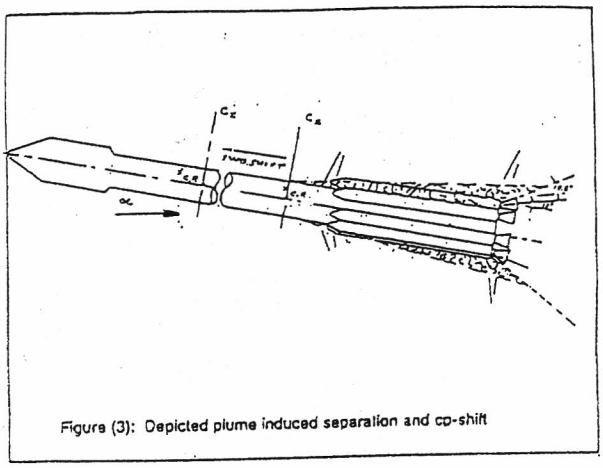

Figure (3): Depicted plume induced separation and cp-shift

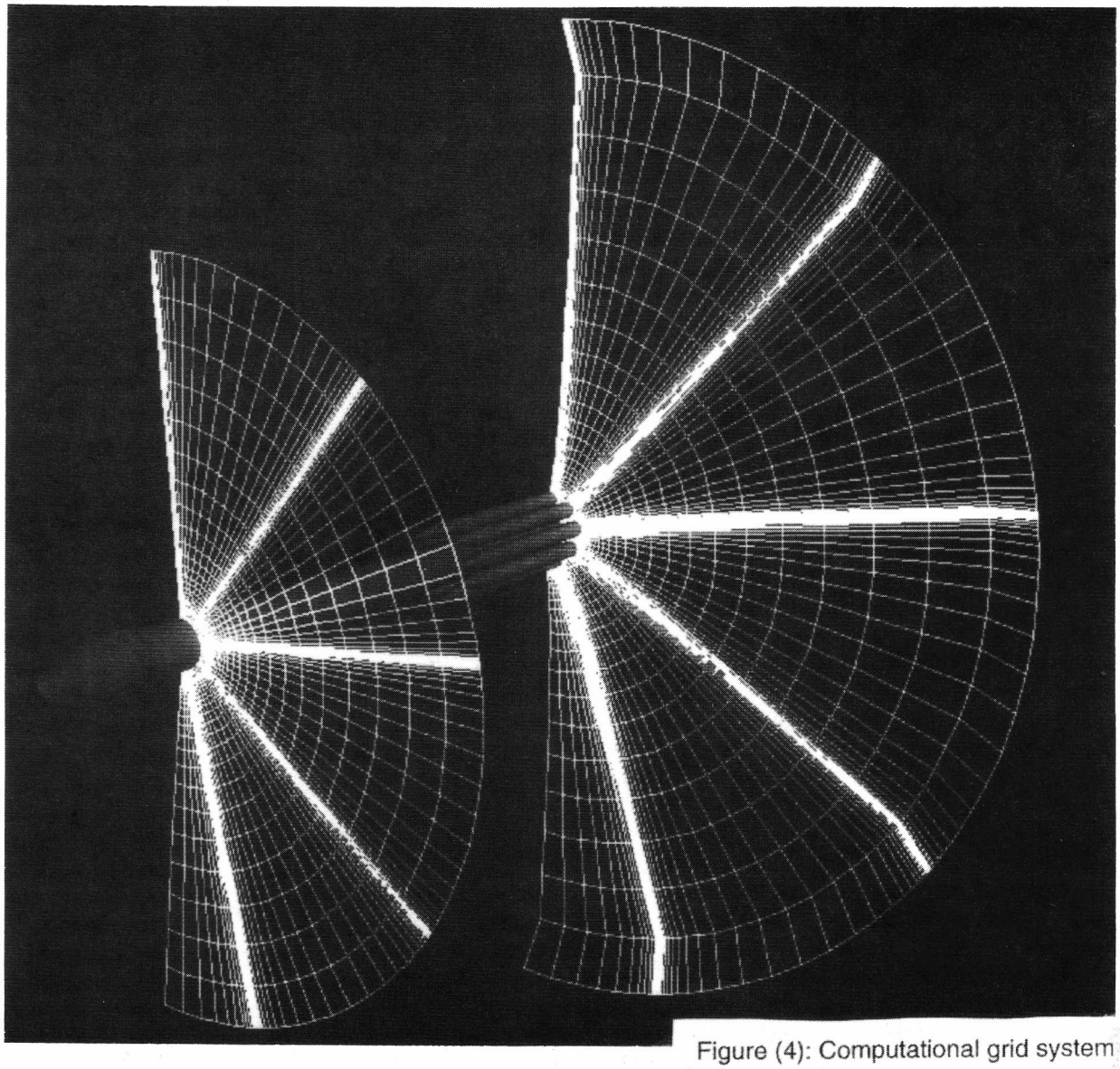

Figure (4): Computational grid system

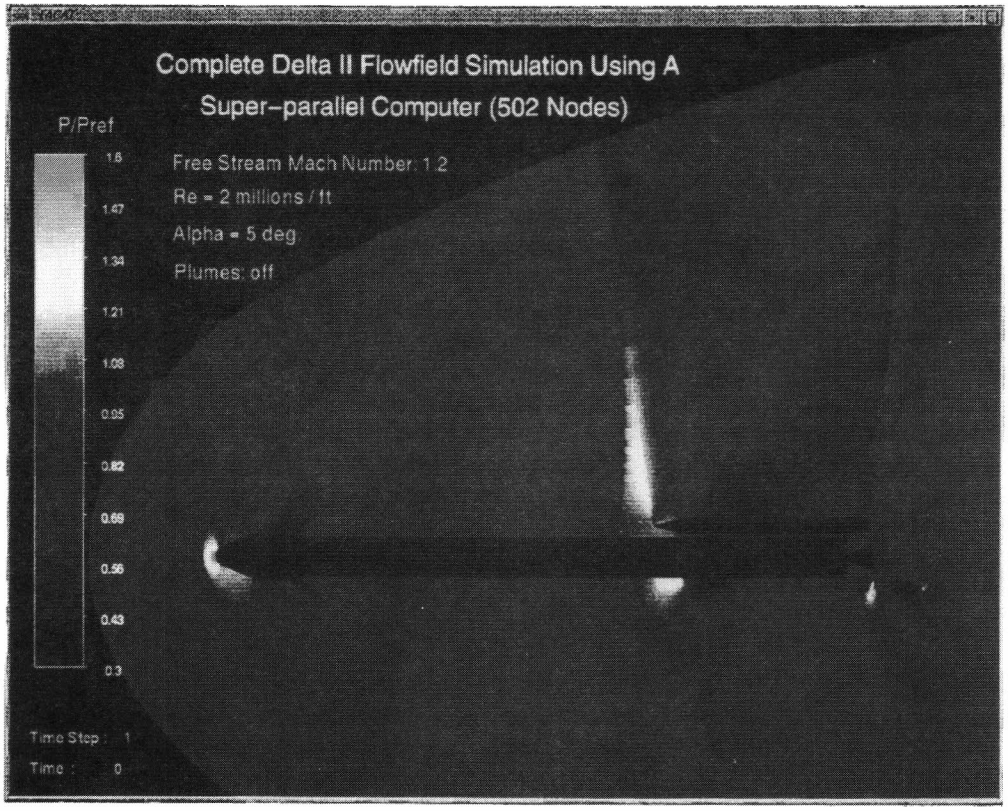

Figure (5a): Pressure contours on the pitch plane of symmetry, plume-off

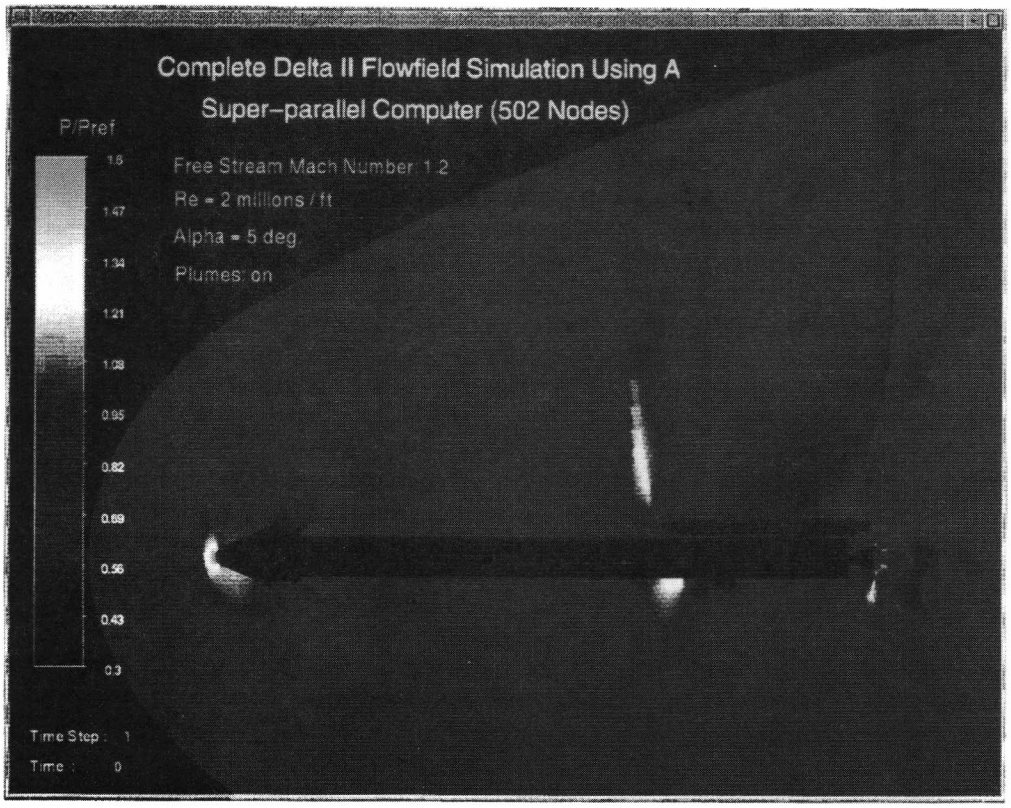

Figure (5b): Pressure contours on the pitch plane of symmetry, plume-on

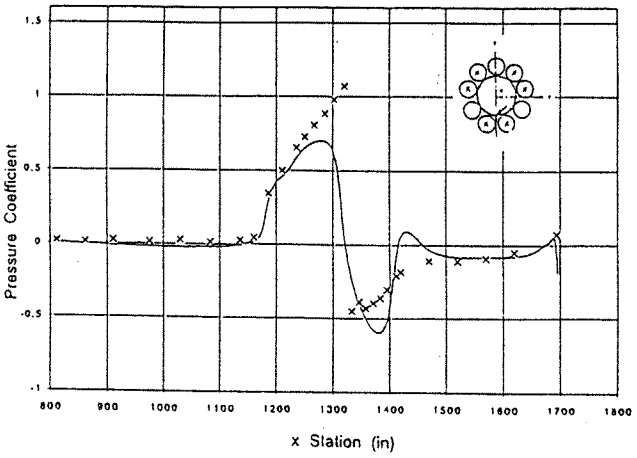

Figure (6a): CFD simulated surfacs pressure (solid line) in comparison with wind tunnel measured data (symbol).

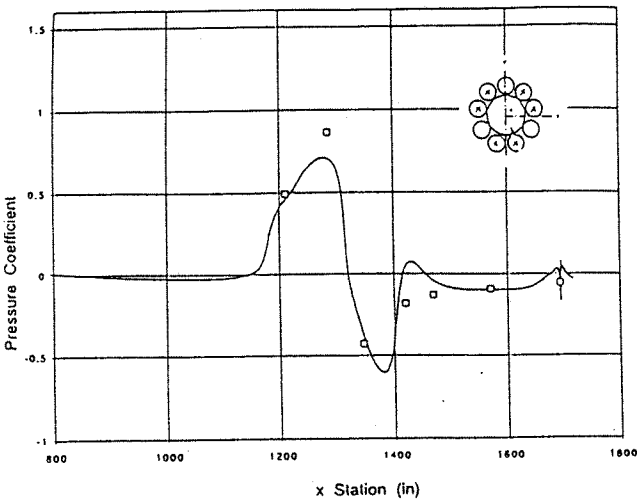

Figure (6b): CFD simulated surfacs pressure (solid line) in comparison with wind tunnel measured data (symbol).

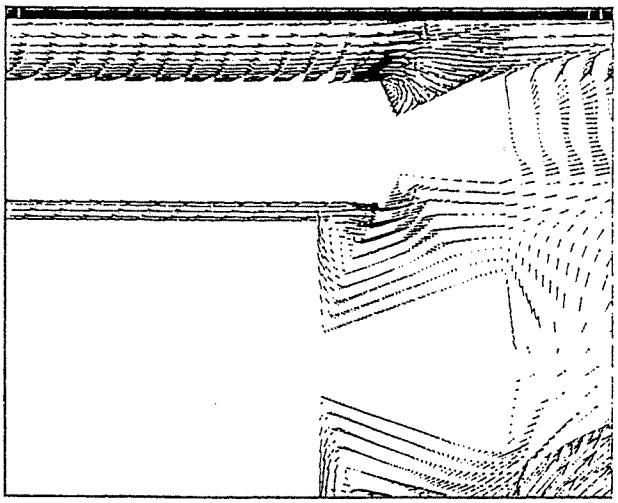

Figure (7a): Velocity vectors on the plane of symmetry, plume-off.

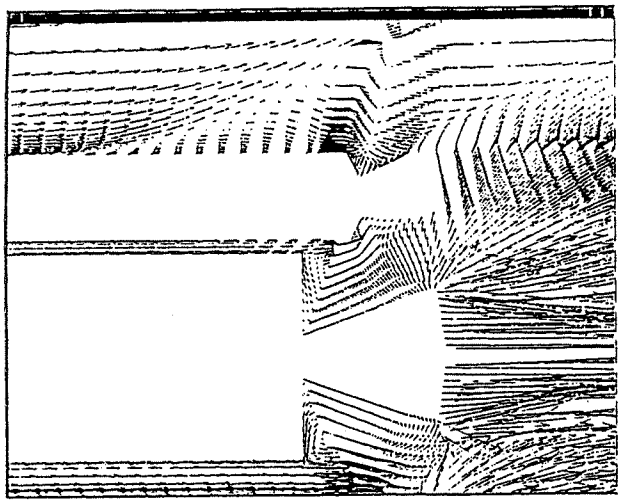

Figure (7b): Velocity vectors on the plane of symmetry, plume-on.

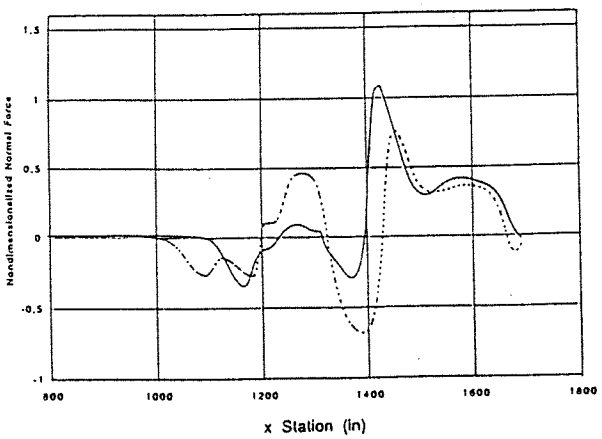

Figure (8): Normal force distribution; —— plume-off, - - - - - plume-On

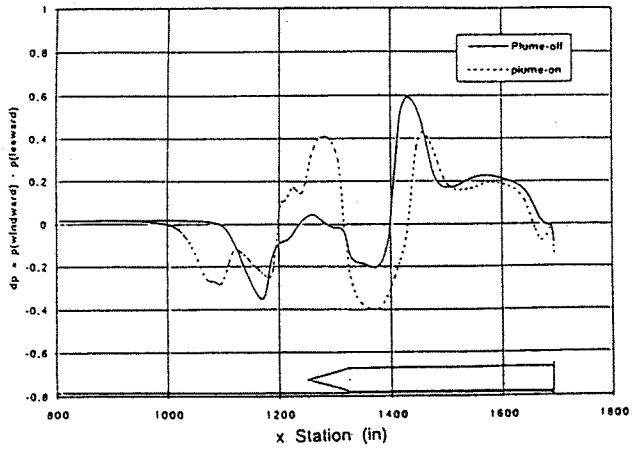

Figure (9): Windward and leeward pressure differential